

PAPER

Microfabricated fiducial markers for digital image correlation-based micromechanical testing of LIGA Ni alloys

To cite this article: Li-Anne Liew *et al* 2021 *Eng. Res. Express* 3 025019

View the [article online](#) for updates and enhancements.

Engineering Research Express



PAPER

Microfabricated fiducial markers for digital image correlation-based micromechanical testing of LIGA Ni alloys

RECEIVED
8 March 2021

REVISED
13 April 2021

ACCEPTED FOR PUBLICATION
23 April 2021

PUBLISHED
5 May 2021

Li-Anne Liew¹ , David T. Read¹ , May L. Martin¹ , Todd R. Christenson² and John T. Geaney³

¹ National Institute of Standards and Technology, Applied Chemicals and Materials Division, Boulder, CO 80305, United States of America

² HT Micro Analytical Inc., Albuquerque, NM 87109, United States of America

³ US Army Combat Capabilities Development Command Armaments Center, Picatinny Arsenal, NJ 07806, United States of America

E-mail: li-anne.liew@nist.gov

Keywords: MEMS, micromechanical testing, electrodeposited nickel, speckle pattern

Abstract

Photolithographically defined thin film Au dots were used as micro fiducial markers for digital image correlation (DIC), to enable two-dimensional strain measurement of 200 μm -thick LIGA (Lithographie, Galvanformung, Abformung) nickel alloys. Due to the sensitivity of electrodeposited films' microstructure and properties on the processing conditions, characterization of LIGA mechanical properties continues to be necessary for microsystems commercialization. DIC offers advantages over laser-based strain measurement techniques but creating suitable speckle patterns on specimens with dimensions under a millimeter is challenging. The material surface roughness itself is often used as the speckle pattern, or micro- or nanoparticles are applied to the surface. But for materials with highly polished surfaces, such as commercial LIGA alloys, the surface roughness is not always suitable, while application of particles still poses technical challenges in uniformity and reproducibility. We fabricated freestanding tensile specimens, with gauge sections 700 μm wide \times 3 mm long \times 200 μm thick, from electrodeposited Ni-10% Co using a commercial LIGA process, and conducted microtensile tests at strain rate 0.001 s^{-1} . Designing and fabricating arrays of randomly oriented 1.5 μm -thick Au dots on the specimens provided a suitable way to obtain full-field surface strains over the entire gauge lengths and was reproducible from one specimen to another. Microfabricated fiducial markers therefore can be a useful surface-preparation approach for investigating micromechanical behavior, particularly plasticity and fracture, of LIGA films using DIC.

1. Introduction

LIGA (Lithographie, Galvanformung, Abformung) is a microfabrication process for manufacturing thick film and high aspect-ratio metal Micro-Electro-Mechanical Systems (MEMS). First developed in the 1980s, LIGA produces electrodeposited nickel structural layers of thicknesses ranging from a few microns to about 1 mm, and thickness-to-width ratios of up to 1000:1 [1–4]. LIGA MEMS devices include micro power relays, micro electromagnetic sensors and actuators, micro optical components, and mold inserts for polymer microfabrication. Due to the wide range of applications ranging from defense to consumer electronics and medical devices, and the well-documented sensitivity of electrodeposited films' microstructure and properties on the processing conditions, MEMS reliability is the subject of much ongoing research and development. This requires ongoing characterization of LIGA alloys' mechanical properties for input into finite element codes and material failure prediction models.

Much work has been done in the past three decades to characterize the mechanical properties of LIGA alloys. Many test techniques have been developed for measuring mechanical properties of materials with characteristic length scales in the nanometer to millimeter range—see, for example, the reviews in [5–7]. Despite the large array of techniques developed, the uniaxial tensile test is still considered the 'gold standard' as it produces uniform strain fields, provides information on fracture behavior, and interpretation of the test data is

unambiguous and straightforward. Experimentally, however, tensile testing of micro- and mesoscale specimens is still fraught with technical challenges that affect the accuracy and reproducibility of the property data. (Here we define the ‘mesoscale’ as gauge section dimensions ranging from tens of microns to a millimeter, as is typical of many LIGA fabricated components). Among these challenges is strain measurement.

Many recent and contemporary works on micro- and meso-scale tensile testing use laser interferometry for strain measurement, such as the interferometric strain/displacement gauge (ISDG) method first developed by Sharpe *et al* [8, 9]. Other researchers have used commercial laser micrometers [10] and commercial infrared displacement sensors [11]. Alternatively, if the specimens are thin films or nanomaterials thus requiring forces in the micro- to pico-Newton range, MEMS actuators may be used to apply the loads, and specimen displacements may be measured in a scanning electron microscope (SEM) by means of on-chip microfabricated vernier scales whose separation is determined by mask design and resolution of the fabrication techniques, a recent example is in [12].

The above approaches, however, are typically limited to one-dimensional strain measurement. In the case of the ISDG approach, specimens can be designed to have ‘tabs’ protruding from the ends of the gauge section to function as targets for the laser and as pre-determined points defining the gauge length [10, 13], in which case attention also needs to be given during specimen design to ensure the tabs do not affect the specimen’s mechanical behavior.

An alternative non-contact strain measurement method that was first established for macroscale mechanical- and civil engineering applications, and which has been gaining interest for micromechanics testing, is digital image correlation (DIC); a comprehensive coverage of DIC fundamentals is in [14] and a recent review was reported in [15]. Currently, DIC with 8-bit grayscale image resolution allows sub-pixel displacement resolution [14]. DIC offers several advantages over laser-based methods: In addition to measuring the engineering strain for constructing load-displacement and stress-strain curves, two-dimensional surface strain maps can be constructed to give more information about the mechanical behavior to predict quantities such as crack initiation and growth. Local strains and strain concentrations can also be measured (limited by the resolution of the images and quality of the specimen surface), which provides an additional advantage of facilitating specimen design. Furthermore, the same set of raw data (images) can be used for all the above. Compared to laser-based approaches for strain measurement, DIC is thus capable of providing an abundance of additional information on mechanical behavior, particularly data relevant to plasticity and fracture.

A key requirement for DIC is the presence of appropriate random surface patterns with sufficient contrast. On macroscale structures in mechanical- and civil engineering applications, this is usually achieved by spray painting to create a speckle pattern. But it is well-known that creating a random isotropic speckle pattern on small specimens is challenging [16], and as such, many studies on MEMS materials do not include any surface preparation for DIC, instead relying on the material’s natural surface texture at the micro- and nanoscale as the pattern. For example, Chasiotis and Knauss used DIC of atomic force microscope (AFM) images to measure strains of surface-micromachined polysilicon tensile specimens fabricated in the commercial Multi-User MEMS Process (MUMPS), using the polysilicon’s surface roughness as the speckle pattern for a portion of the gauge section [17]. Roland *et al* [18] used DIC to measure strains and local deformations of Au and Pt thin films deposited on 200 μm -thick SU8 photoresist polymer, using the metal film’s microstructural surface features as the speckle pattern.

Other researchers have explored various approaches to create speckle patterns. For example, Robin *et al* [19] used DIC to obtain stress-strain curves for 2 μm -thick polymer films. The tensile specimens were mesoscale, with gauge dimensions of 900 $\mu\text{m} \times 400 \mu\text{m}$, and copper oxide microparticles were applied to the surface by air blowing to create the speckle pattern. Naraghi *et al* [20] used surface micromachined polysilicon MEMS actuators to perform on-chip tensile tests of ductile nanofibers. To create the pattern for DIC, they used focused ion beam milling (FIB) to etch circular patterns a few tens of nanometers deep and with diameters ranging from sub-microns to microns. Jonnalagadda *et al* [21] did tensile tests on Pt thin films with silicon microparticles applied to the surface for DIC. Banks-Sills *et al*. [22] performed tensile tests of single-crystal silicon specimens with gauge dimensions in the tens of microns, and applied carbon black to the silicon surface to create the speckle pattern, but the pattern was suitable for DIC only on some regions of the gauge section. Other methods include rearrangement of chemical vapor-deposited thin films [23], and e-beam lithography [24].

Berfield *et al* [25] did a study on different means of producing speckle patterns for DIC at different size scales, to enable micro- versus nanoscale deformation measurements of transparent polymer specimens. They used airbrushing for the microscale polymer specimens with an image resolution of 3 to 10 $\mu\text{m pixel}^{-1}$, and a solution of fluorescent nanoparticles for nanoscale specimens with image resolutions of 134–213 nm pixel^{-1} .

Photolithography has also been used to create speckle patterns for DIC. Scrivens *et al* [23] directly deposited and patterned thin film micro-speckle patterns directly on the surface surrounding the crack tip of a 2 mm-thick metal CT specimen, while Ruggles *et al* [26] developed a microstamping technique in which elastomers cast into

photolithographically fabricated molds were used as flexible stamps for imprinting the mold pattern onto silicon for DIC imaging in an SEM.

Most studies to date on LIGA materials, however, used laser-based methods for strain measurements in microtensile tests. But among those that used DIC, Collins *et al* [27] did not do any surface preparation of their LIGA Ni tensile specimens, instead relying on the specimens' surface roughness. Sharon *et al* [28] tested 10 μm -thick nanograined Ni-Fe with a 2 mm-long gauge section, by applying 3–9 μm -diameter toner particles to the surface to create the speckle pattern. Suresha *et al* [29] used DIC to measure strains in tensile tests of LIGA Ni-W specimens of gauge size similar to the present study, but did not discuss surface preparation methods, if any. These studies did not include full-field strain mapping over the *entire* length of the gauge sections. A possible reason could be the fact that achieving a DIC-suitable speckle pattern over an entire microscale specimen, and reproducing such a pattern reliably over many specimens, is challenging when using particles and the surface roughness.

We recently reported the elastic-plastic properties of two LIGA Ni alloys fabricated in a commercial process by HT MicroAnalytical, Inc. [30, 31]. Since the specimen surfaces were highly polished and devoid of features when the whole gauge section is viewed under an optical microscope, speckle patterns had to be created on the surfaces to enable strain-measurement by DIC. In this paper, we compare several techniques for creating the speckle patterns for two-dimensional strain mapping. These techniques can be broadly divided into two categories: post-fabrication surface preparation, and *in situ* wafer-level fabrication of a microengineered speckle pattern on the surface of the LIGA specimens as the last step of the fabrication process before releasing the specimens from the wafer. We then discuss the uncertainty in our DIC techniques and compare results from two specimens of the same material and geometry, one with the microfabricated pattern and one decorated with SiC particles on the surface. We show that the two-dimensional strain maps produced from the *in situ* microfabricated pattern were of higher quality and reflected the expected specimen behavior. Furthermore, compared to the particles approach, the microengineered pattern resulted in more repeatable and uniform strain fields, and allowed repeatable strain mapping of the entire 3 mm long \times 700 μm wide gauge section.

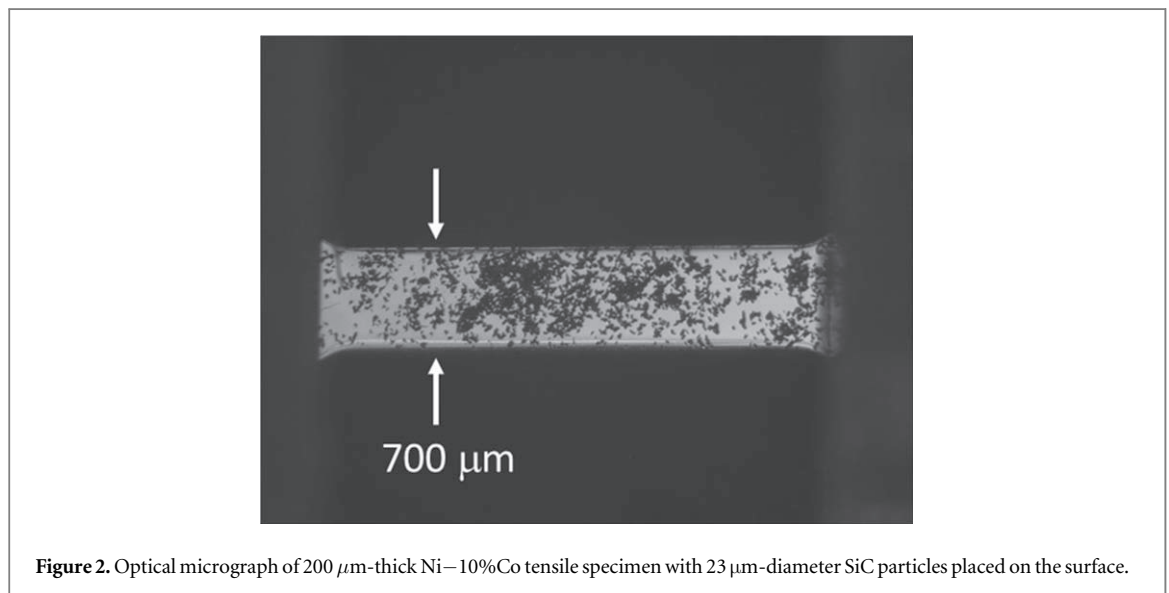
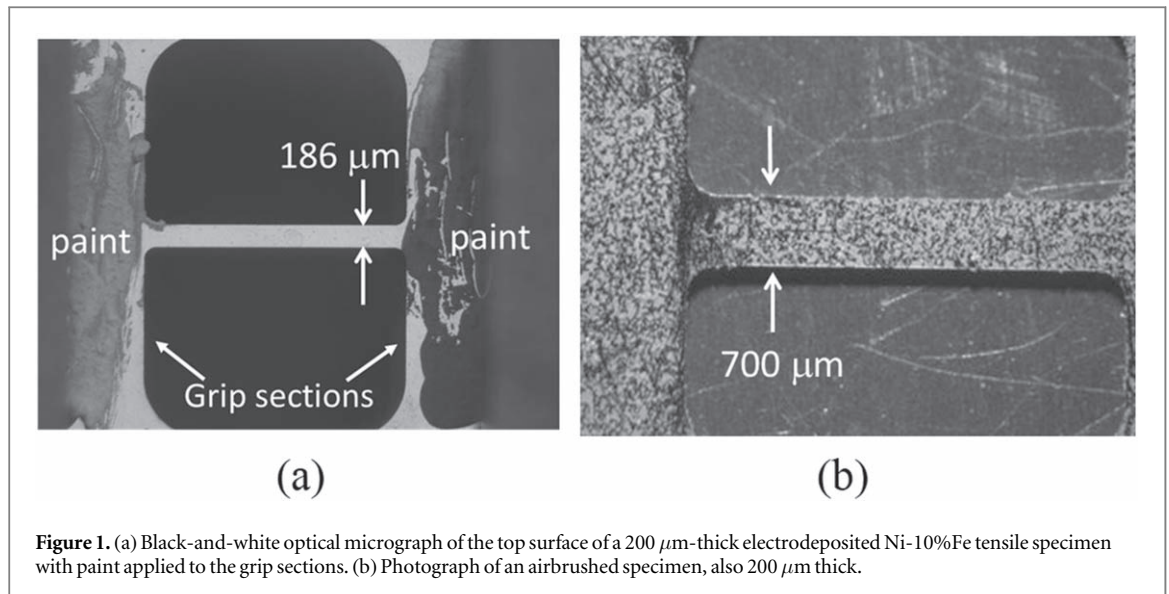
2. Materials and methods

2.1. Specimen design, and post-fabrication surface modification approaches

200 μm -thick specimens of a Ni-10% Co alloy were fabricated in a commercial LIGA process, and were tensile tested at strain rates 0.001 s^{-1} under an optical microscope with a 2X objective lens. Details of the specimen design, fabrication process, material microstructure, chemistry and elastic-plastic properties are in [30, 31], while details of the material's fracture mechanisms are in [32]. In this paper, we focus on the specimens with gauge dimensions of 700 μm wide \times 3 mm long. The as-fabricated specimens possessed smooth and highly polished mirror-like surfaces characteristic of commercial LIGA processes. To enable strain measurement by use of DIC, the surfaces required a fixed and random pattern of contrasting dark and light regions. We explored several techniques for creating patterns before selecting the microengineered fiducial markers approach for our test campaign in the above references. We now described the surface patterning approaches.

The first approach consisted of applying dilute water-soluble white paint using a fine wire, shown in figure 1(a). Paint was applied only to the specimens' grip sections but not to the gauge sections. The unevenness of the paint layer provided sufficient contrast in the optical microscope images such that DIC could be done on two regions—one at each grip section—to measure the engineering strain. While this was adequate for constructing engineering stress-strain curves, it was not applicable to obtaining full-field strains due to difficulty in applying the paint to the smaller and more fragile gauge sections without influencing the mechanical properties due to the paint layers' difficult-to-control thickness. We also explored the use of airbrushing, whereby we first airbrushed a layer of black paint on the specimen surface to reduce the reflectivity, followed by airbrushing a layer of white paint to provide contrasting patterns against the background, see figure 1(b). While this allowed two-dimensional DIC to be performed across the gauge sections, again the drawback was difficulty in reliably controlling the thickness of the paint such that it would not influence the measured mechanical response of the specimen. Furthermore, it was also difficult to control the evenness of the airbrushed layers on these small specimens, which would lead to varying image quality from one specimen to another.

In a third preliminary approach, we used a fine wire to place drops of isopropyl alcohol or deionized water on the gauge sections followed by sprinkling 400 grit (23 μm diameter) silicon carbide (SiC) particles, such that when the liquid evaporated the SiC particles remained loosely adhered to the specimen surface by electrostatic and Van der Waals forces, see figure 2. This approach resulted in greater reproducibility of the contrast in the images from one specimen to another and reduced the potential of affecting the mechanical response of the specimen. However, as mentioned by Robin *et al.* [19], a challenge when applying micro-particles to mesoscale specimen surfaces is achieving a uniform density of the particles (preventing agglomerates) across the entire



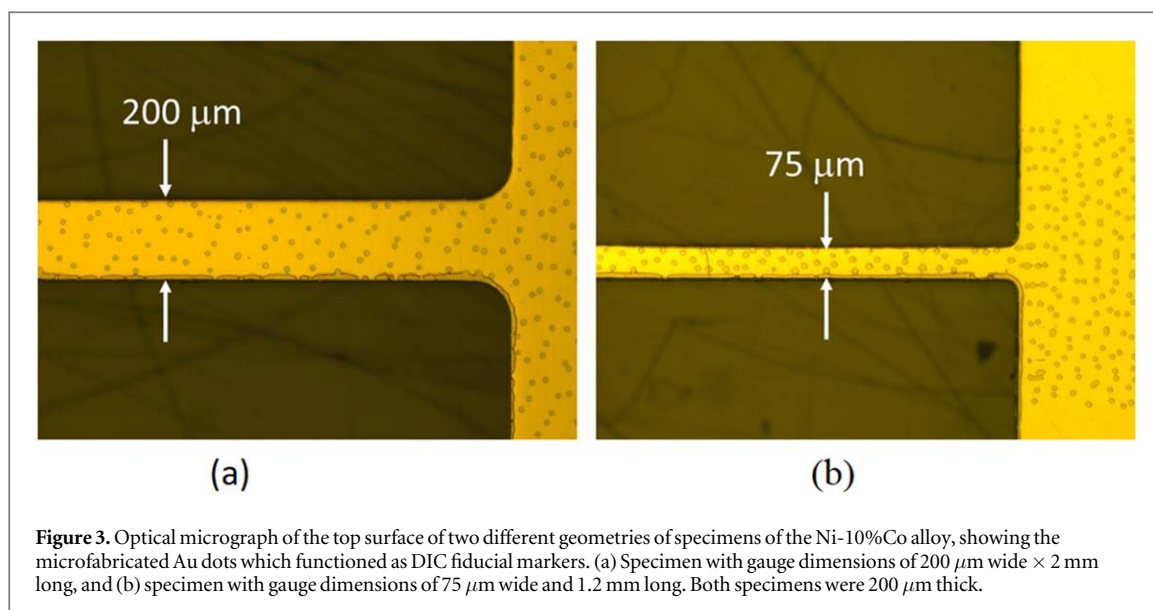
surface while still maintaining adequate randomness of the pattern. It has also been observed that on smaller (thin film) specimens the microparticles tend to form agglomerates [21].

The SiC powder worked well for measuring engineering strain at strain-rate 0.001 s^{-1} . However, reproducibility of the pattern quality over the whole gauge section and from one specimen to another was challenging, making two-dimensional strain measurement unreliable. This approach was also problematic for testing at higher strain rates in a different test set-up. Unlike in the 0.001 s^{-1} test apparatus where the specimens were positioned horizontally in the test frame, specimens were held vertically in the higher rate set-up and thus required considerably more maneuvering to insert into the load frame. This additional handling caused many SiC particles to fall off the specimens. Details of our experimental set ups and test procedures are in [30, 31].

2.2. Microengineered fiducial markers

While each of the above initial surface preparation methods met with some degree of success for measuring the engineering strain from the ends of the gauge sections, which is all that is needed to extract stress-strain tensile behavior, extending the DIC to two dimensions over the whole gauge section led to highly uncertain and varying results.

We found that a reliable method for two-dimensional strain mapping was photolithographically fabricating a layer of thin-film Au fiducial markers on one surface of the specimens, as shown in figure 3. Each Au dot was $1.5 \mu\text{m}$ thick and $25 \mu\text{m}$ wide, as measured by profilometry. The dots were deposited and patterned at the wafer-level as the final step in the LIGA fabrication process, but before the specimens were released from the wafer. By



creating the dots directly in the photolithographical mask, the pattern and optical contrast is replicated exactly for all specimens, thus ensuring reproducibility of the DIC over the whole gauge section and across all specimens. CAD techniques used in mask design were used to engineer the pattern precisely by controlling the size, spacing and orientation of the fiducial markers to achieve sufficient randomness and contrast for DIC, and the pattern density can be tailored to different desired strain resolutions and different specimen geometries. For example, the pattern can be made denser in regions where higher spatial resolution is desired, being limited by the Rayleigh criterion of $\lambda/2$ where λ is the wavelength of the light. (For visible light, this limit would be ~ 200 nm.) We used two methods to design the pattern, one involved creating linearly increasing helical spirals and overlaying them, and another involved using an algorithm to create small rectangles of random orientation and spacing. Since the Au layer is two orders of magnitude thinner than the specimen, the fiducial markers have negligible effect on the specimens' mechanical behavior.

Another advantage over our earlier surface preparation approaches is that the specimens did not require post-processing after release from the wafer since the pattern is fabricated *in situ* during the commercial LIGA manufacturing process. Eliminating the need for post-processing on free-standing mesoscale specimens is desirable as any post-processing could potentially damage or scratch the fragile gauge sections or alter the mechanical properties through slight unintended pre-loading. (However, if the specimens were not made in a wafer-scale microfabrication process, post-fabrication deposition of the Au pattern could in principle still be achieved through a shadow mask to create these same microengineered fiducial markers on the surface). While the dots are randomly distributed within a pattern on a specimen, the patterns are replicated for each specimen of the same geometry. This leads to repeatability of the DIC parameters from one specimen to another. (We had tested about 50 specimens in our earlier work [30–32].)

Figure 4 shows typical optical micrographs taken during a tensile test, with the DIC grid overlaid. The Au dots appear darker than the bare Ni under direct illumination (figure 3), while under oblique illumination the dots appear brighter (figure 4). This optical contrast under both types of illumination is likely due to diffuse reflection from the Au surface and specular reflection from the highly polished Ni surface. Figure 4(c) shows a single DIC subset of 80 pixels on the same specimen from (a) and (b).

2.3. Tensile testing and digital image correlation

The specimens were tensile tested using a commercial miniature tensile test stage with custom clevises. The tests were done at a strain rate of 0.001 s^{-1} under an optical microscope with a 2X objective lens, with a CCD camera capturing images of the gauge section at a rate of 1 image per second. The size of each image was 3072×2300 pixels which corresponded to a resolution of about $1.4 \mu\text{m pixel}^{-1}$. Details of the test apparatus and the test and analysis procedures are reported in [30, 31]. In that study, a total of 48 specimens—which included three more specimen geometries, an additional higher strain rate, and one additional LIGA alloy—were tested, all had the microfabricated fiducial markers for DIC. While the results presented in this paper are from only one material and geometry, the results from the total number of tests in the study gives us confidence in this technique. The specimen with microengineered fiducial markers described in the next section was among those tested in that study and was tested at strain rate 0.001 s^{-1} .

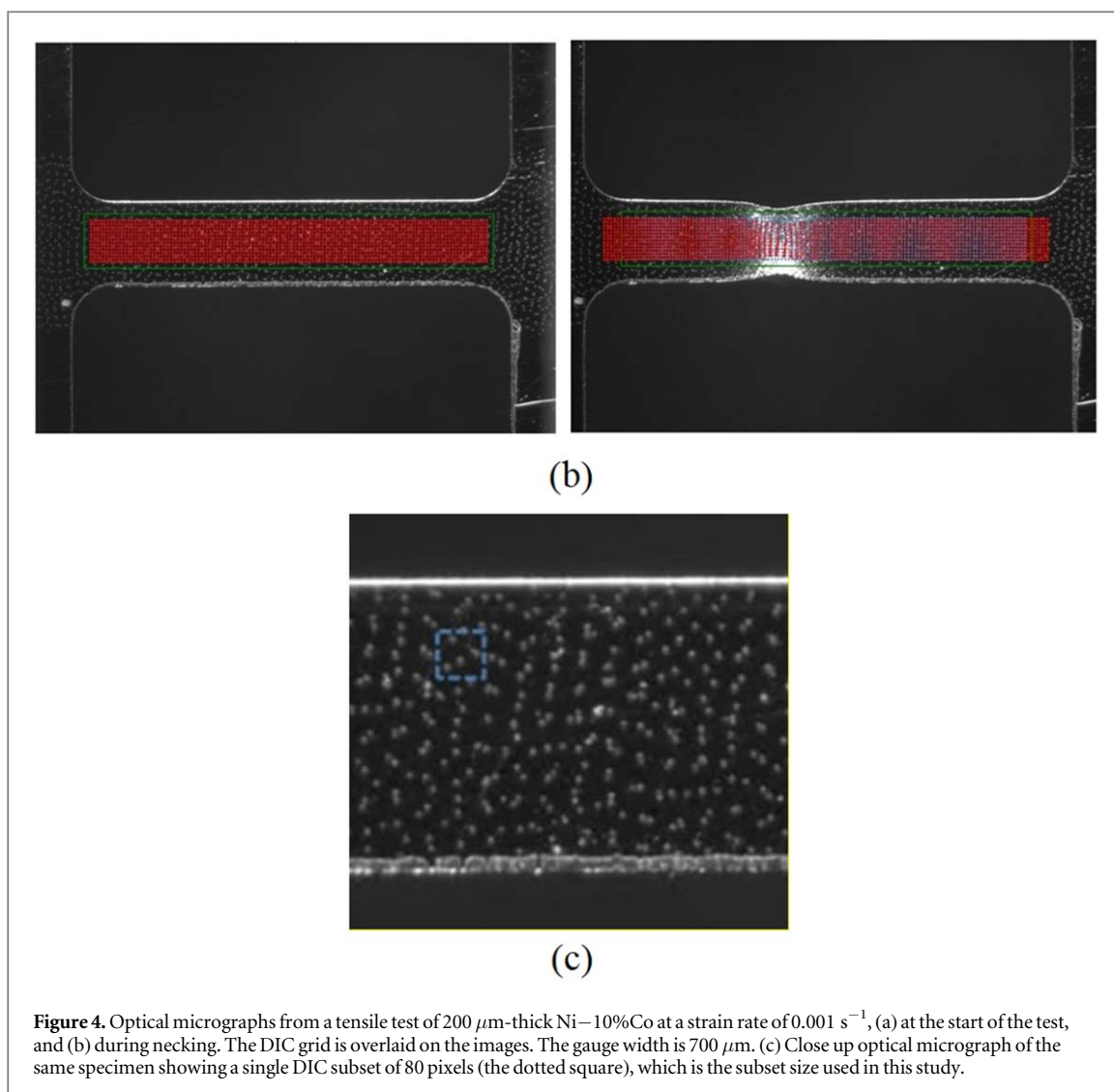


Figure 4. Optical micrographs from a tensile test of 200 μm -thick Ni–10%Co at a strain rate of 0.001 s^{-1} , (a) at the start of the test, and (b) during necking. The DIC grid is overlaid on the images. The gauge width is 700 μm . (c) Close up optical micrograph of the same specimen showing a single DIC subset of 80 pixels (the dotted square), which is the subset size used in this study.

After testing, the images were analyzed offline using a custom DIC program which we used in our previous work [30, 31]. The program allowed individual subsets or arrays of subsets to be tracked. The output was a spreadsheet of raw displacements, which were then separately analyzed to calculate the strains.

We confirmed the efficacy of our DIC program down to a strain of 0.001, as follows: we took already-acquired images of a specimen which had not been tensile-tested (in this case an airbrushed specimen that was not included in the test campaign of 48 specimens as it did not have the microfabricated dots), and stretched the images by a known amount, thus creating a simulated known strain. We then analyzed the stretched and original images to obtain the ‘apparent strain’ from our DIC program and compared it with the known amount of simulated strain. The original image was imported into the free ImageJ software [33] and stretched from 3072 pixels to 3078 pixels, corresponding to a simulated strain of 0.001953. This new image was then cropped to the same size as the original image, which was 3072×2300 pixels. DIC was then performed between these two images, using both a commercial DIC software (VIC-2D [34]) and our custom program, and compared to the known simulated strain. For an imposed simulated strain of 0.001953, our program produced an apparent strain of 0.001951 and 0.001955 for subset sizes 80 and 120 pixels, while the commercial program produced a strain of 0.001943 and 0.001947 for the same subset sizes. Repeating this exercise with an imposed simulated strain of 0.000970 resulted in a DIC apparent strain of 0.000975 using our program. We therefore conclude that our DIC techniques on the present mesoscale tensile specimens should be accurate to 0.001 strain. In constructing engineering stress-strain curves we do also obtain strains below 0.001, but we consider these low strains to be less accurate. This limitation of our DIC methods adds to the general well-documented difficulties in the mechanical testing communities in obtaining reliable values of the Young’s modulus from the tensile tests; the error analysis is discussed as follows.

Engineering strain is defined as du/l , where du is the change in length of the gauge section (the difference in measured displacements at the ends of the gauge section) and l is the original gauge length. The uncertainty in

the engineering strain is therefore calculated by adding in quadrature the relative uncertainties in du and in l . Both du and l are measured in pixels from the optical micrographs.

The absolute uncertainty in du is taken as 0.2 pixels, which corresponds to about $0.28 \mu\text{m}$. This value is a conservative estimate which we originally derived for tensile tests using cameras and microscopes similar to those used in the present tests, and is similar in value to that reported by other researchers for strains in micro- and nanoscale specimens of other materials [17, 25]. Banks-Sills *et al.* [22], however, reported an absolute uncertainty in du of only 0.005–0.01 pixels when using commercial DIC software to analyze optical micrographs of regions of the silicon tensile gauge sections where the speckle pattern (created by applying carbon black) was suitable for DIC. The relative uncertainty in du is then the absolute uncertainty in du (0.2 pixels) divided by the absolute value of du , which increases with increasing strain.

The relative uncertainty in l is the absolute uncertainty in l (taken as the DIC subset size) divided by the absolute value of l which is ~ 2000 pixels for these tests. While the strain resolution = the absolute uncertainty in du (0.2 pixels)/ l (2000 pixels) = $1\text{E-}4$ strain, the strain uncertainty by definition will vary with the strain. The larger the strain, the smaller the strain uncertainty. The longer the gauge length, the smaller the strain uncertainty because du will be larger for the same strain. For the small strains in the linear elastic region, the strain uncertainty is therefore higher than for strains after yielding. In these experiments, the strain uncertainty varies from 16% at engineering strain of $5\text{E-}4$ which is in the linear elastic region, to 3% at engineering strain of 0.07 corresponding to the ultimate tensile strength. But for the shorter (1.2 mm long) specimens in our previous work [30, 31] the strain uncertainty at engineering strain of 0.07 is about 10%. The subset size also influences the strain uncertainty, as mentioned above. The dependence of the strain uncertainty on the strain and gauge length is characteristic of strain measurement using DIC, with the size of the uncertainty being dependent on the absolute uncertainty in du (which we estimate at 0.2 pixels).

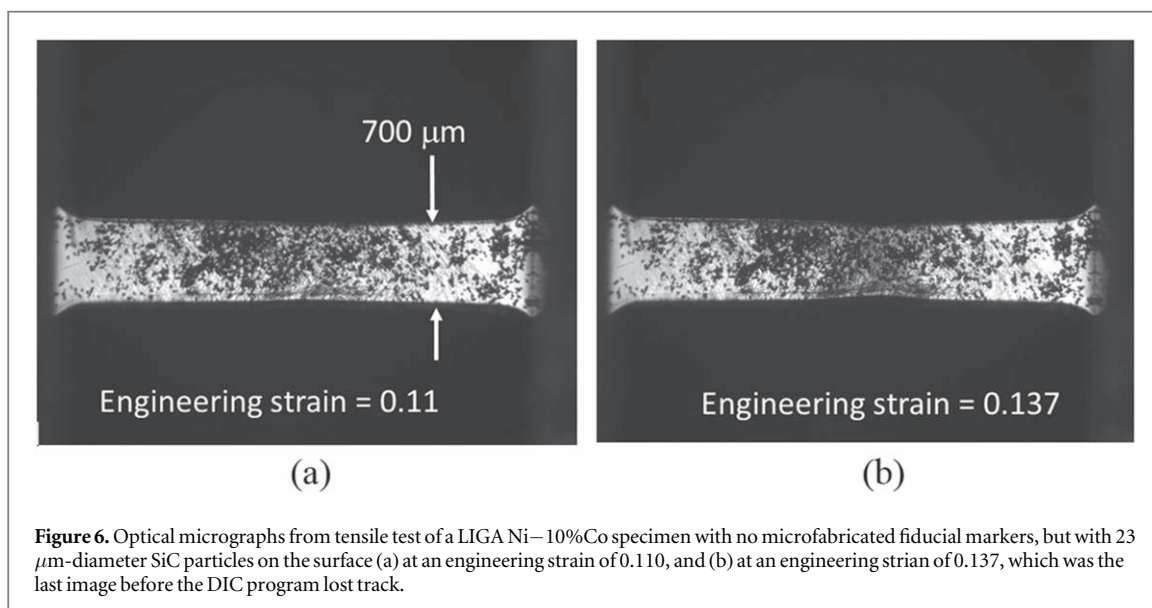
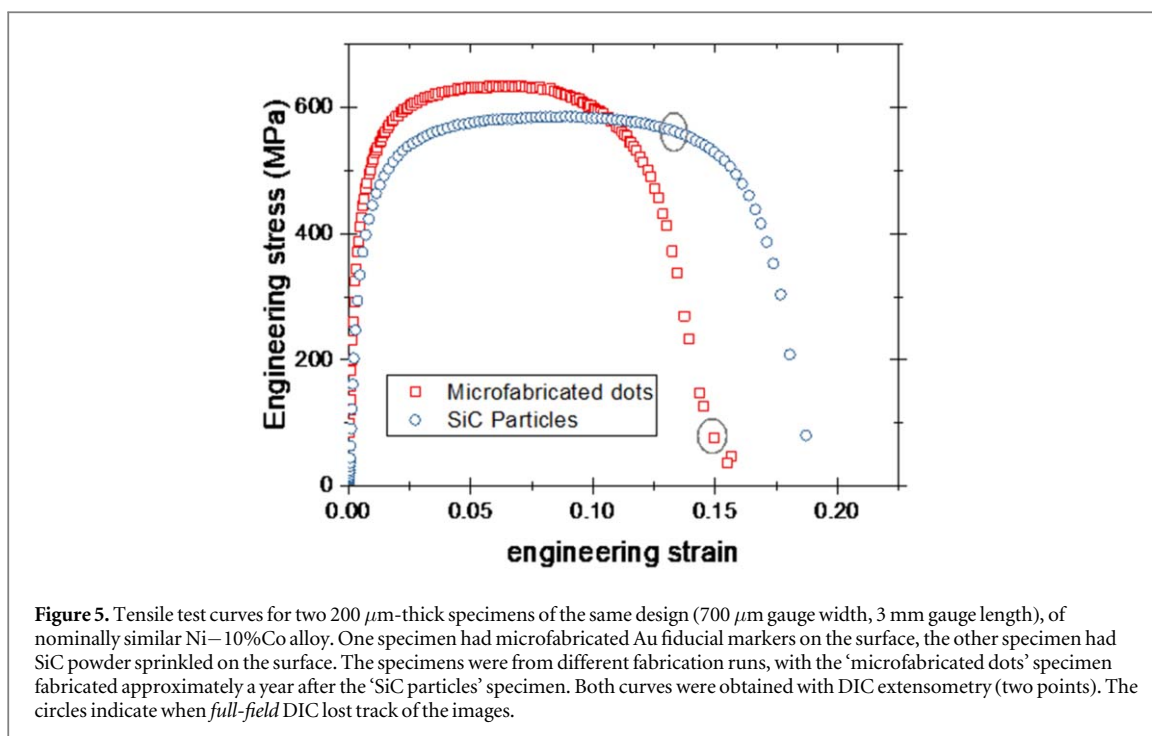
These uncertainties in the strain will also affect other measured values that depend upon the strain measurement, such as Young's modulus. The uncertainty in Young's modulus will depend upon uncertainties in the cross-sectional area measurement, in the force measurement, and in the strain measurement. For this material and in this geometry, it was found that the relative uncertainty in the modulus was 16%, almost entirely due to the relative uncertainty in du [30, 31], when using an absolute uncertainty in du of 0.2 pixels which, as we noted above, is comparable to other studies in the literature.

Noise in the images can arise from relative motions between the camera and the specimen, such as due to drifting of the microscope stage, or camera, or shifting of the specimen out of plane during the test. We found these factors to be negligible in our tests at the magnifications used. For our experimental set up, a spurious strain of ± 0.001 would be produced if the specimen were to be moved $\sim 250 \mu\text{m}$ above or below the initial focus position. Moving the specimen closer to the lens makes it appear bigger, resulting in a positive spurious strain. A noticeable defocusing of the image is perceptible at $\sim 150 \mu\text{m}$ of movement away from the initial plane of focus under the 2X objective lens used for all tests. Under a 10X objective lens a noticeable defocusing of the image occurs at $\sim 25 \mu\text{m}$ of vertical motion out of the focal plane. Yet when we tested a specimen under the 10X objective, we did not perceive any defocusing of the images. We thus conclude that the strains measured from the images (taken with the 2X objective lens during tensile tests) are relatively unaffected by any extraneous motions or drifting of the test apparatus.

3. Results and discussion

Figure 5 compares the engineering stress-strain curve of two $200 \mu\text{m}$ -thick specimens of the same design (gauge dimensions $700 \mu\text{m}$ wide \times 3 mm long) of the Ni-10%Co alloy. One specimen had the microfabricated pattern on the surface, the other had SiC particles applied to the surface. It has been well-documented in the literature that the chemistry, microstructure, and properties of electrodeposited metals are highly sensitive to the plating conditions such as bath chemistry, pH, temperature, amount of agitation, etc. Since the two specimens in figure 5 were fabricated in different fabrication runs spaced approximately a year apart, it is not unusual that their mechanical properties differ.

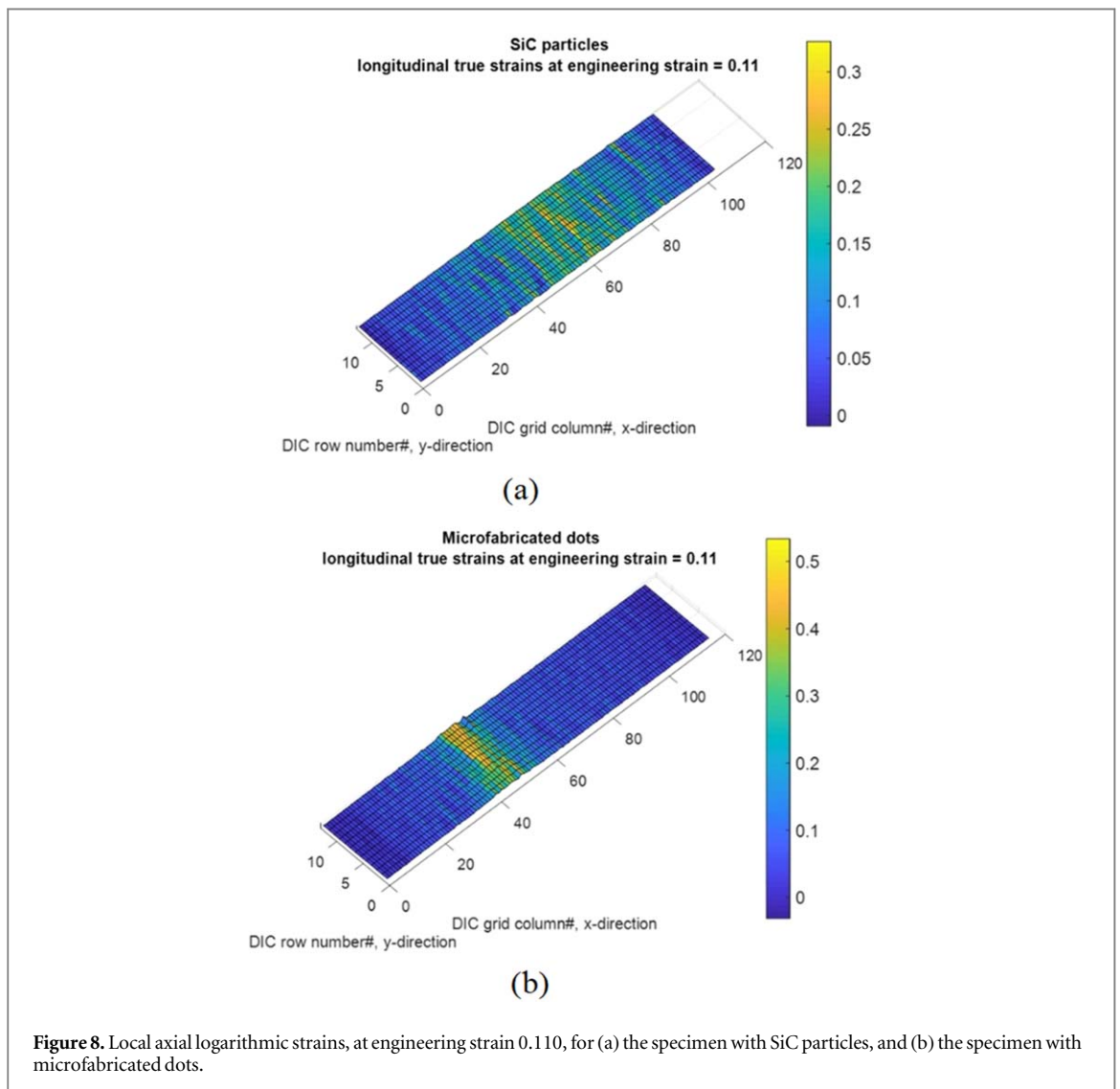
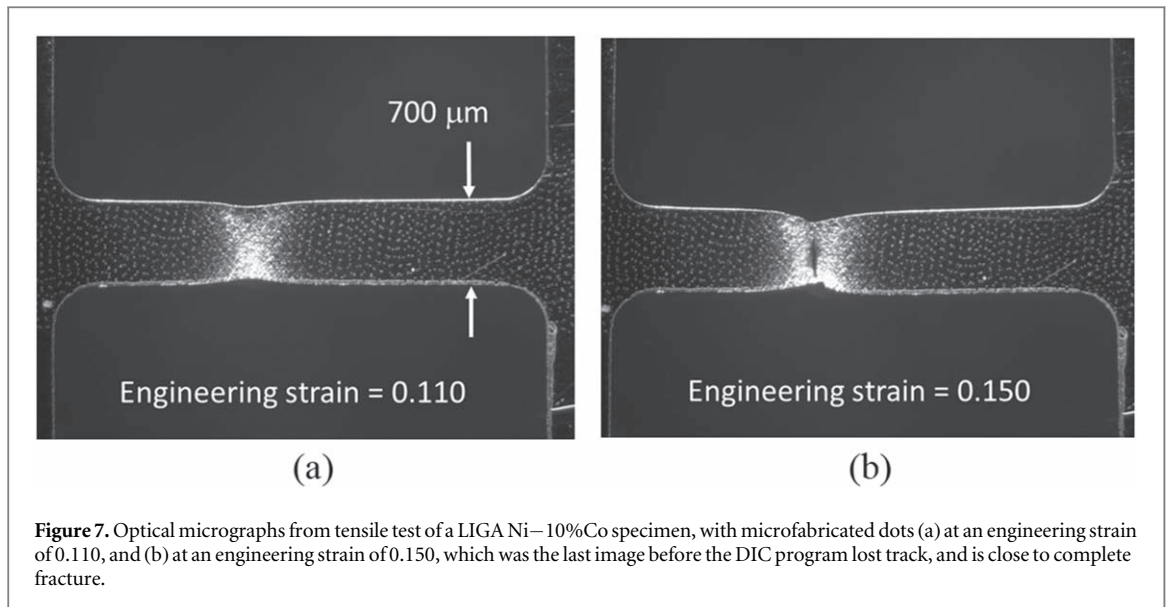
While the engineering stress-strain curves for each specimen in figure 5 were obtained by using only two points for the DIC (one at each end of the gauge section like an extensometer), for obtaining two-dimensional surface strain fields, we used an array of subsets spanning the whole gauge section, as shown in figure 4. A typical $700 \mu\text{m} \times 3 \text{ mm}$ gauge length spanned about 2300 pixels in length. The calibration factor for the microscope with the 2X objective is $\sim 1.4 \mu\text{m pixel}^{-1}$. With a DIC subset size of 80, subdivided by 4 (i.e. 20 pixels), this results in the size of each subdivided subset region being 28 microns long. For a gauge width of $700 \mu\text{m}$, this corresponds to each subdivided subset region (28 microns) being about 4% of the gauge width.



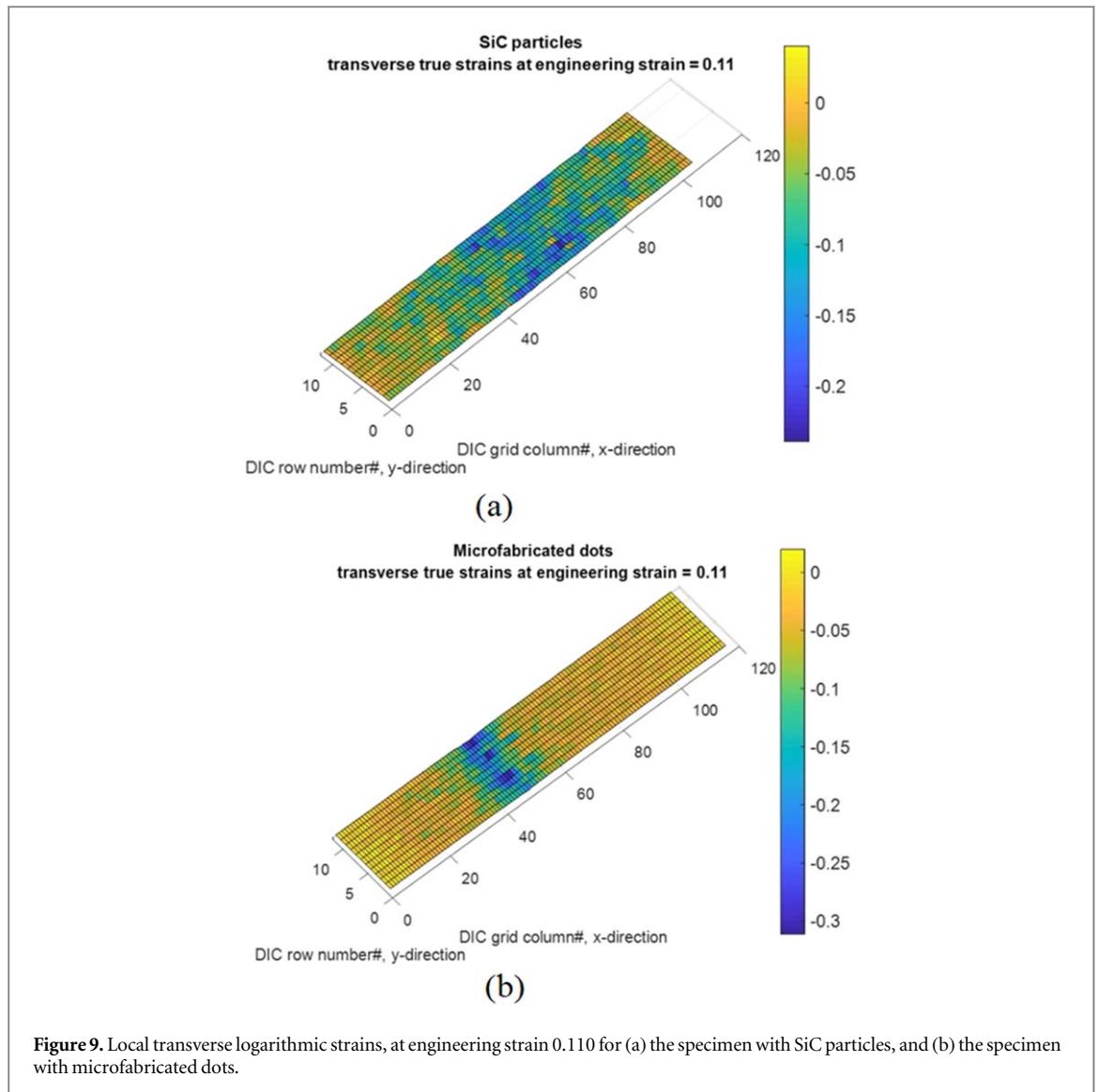
We re-analyzed the same images that were used to construct the stress-strain curves of figure 5, but now with arrays of subsets covering the whole gauge sections. From the DIC program’s output of raw displacements, the local true or logarithmic strains in the longitudinal and transverse directions were computed.

The engineering stress-strain curves (figure 5) show that the ‘SiC Particles’ specimen was more ductile. However, when full-field DIC was performed on the same images, the program lost track of the particles about two thirds of the way into the sequence of images, corresponding to an engineering strain of about 0.137. Thus, for the ‘SiC Particles’ specimen in figure 5, we were unable to obtain full-field surface strains at larger deformations just before fracture. For the ‘microfabricated dots’ specimen, on the other hand, the program was able to track all fiducial markers up until the second-to last image before fracture, corresponding to an engineering strain of 0.150.

Figures 6 and 7 show optical micrographs from the tensile tests of both specimens from figure 5, at engineering strains of 0.110 and at the last images that could be analyzed with the two-dimensional DIC. As shown in this figure, the program was able to track the ‘microfabricated dots’ specimen to a much larger local true strain and degree of necking than for the ‘SiC particles’ specimen.



Figures 8 and 9 show the two-dimensional surface strain fields constructed from the optical micrographs in figure 6(a) and 7(a) above, *i.e.* corresponding to an engineering strain of 0.110 (from figure 5). The strain plotted here is the Hencky strain, also known as the true strain or logarithmic strain [35]. Figure 8 plots the true strain in



the axial direction and figure 9 plots the true strain in the transverse direction. This figure shows that the ‘microfabricated dots’ specimen produced a more uniform strain field in the regions where strain uniformity is expected, that is, outside of the neck, while the ‘SiC particles’ specimen appears to have many regions of spurious strains. One reason for these spurious strains could be that the SiC particles could have shifted position or joined together during the tensile test at the larger deformations since they were only loosely adhered to the surface by electrostatic and Van der Waals forces.

Figures 10 and 11 compare the distribution of local axial and transverse logarithmic strains for the same two specimens side by side, at the last image that could be analyzed by the DIC program. This corresponded to an engineering strain of 0.137 for the ‘SiC particles’ specimen, and engineering strain of 0.150 for the ‘microfabricated dots’ specimen. These are the strain fields constructed from the optical micrographs in figures 6(b) and 7(b) above. Again, the ‘microfabricated dots’ specimen produced more uniform strain distribution in the regions where uniform strain is expected. Furthermore, for the ‘microfabricated dots’ specimen the DIC program was able to track the displacements to much larger deformations.

Therefore, for two specimens of the same nominal material (micrograined Ni-10% Co alloy) and of the same geometry, tested in the same test set up and analyzed with the same DIC program, the microengineered fiducial markers enabled the DIC program to track the full-field displacements to larger strains and more severe deformation than the SiC particles. In fact, the microfabricated dots specimen could be strain-mapped up until 2 images before complete fracture, at an engineering strain of 0.150, when the specimen was already tearing apart at the neck region. The specimen with the SiC particles, on the other hand, could only be analyzed to an engineering strain of 0.137, while the sample was still undergoing necking. Furthermore, when both specimens were examined at engineering strain of 0.110, the microfabricated Au pattern produced much more uniform strain distribution in regions outside the neck, as expected, than the SiC particles.

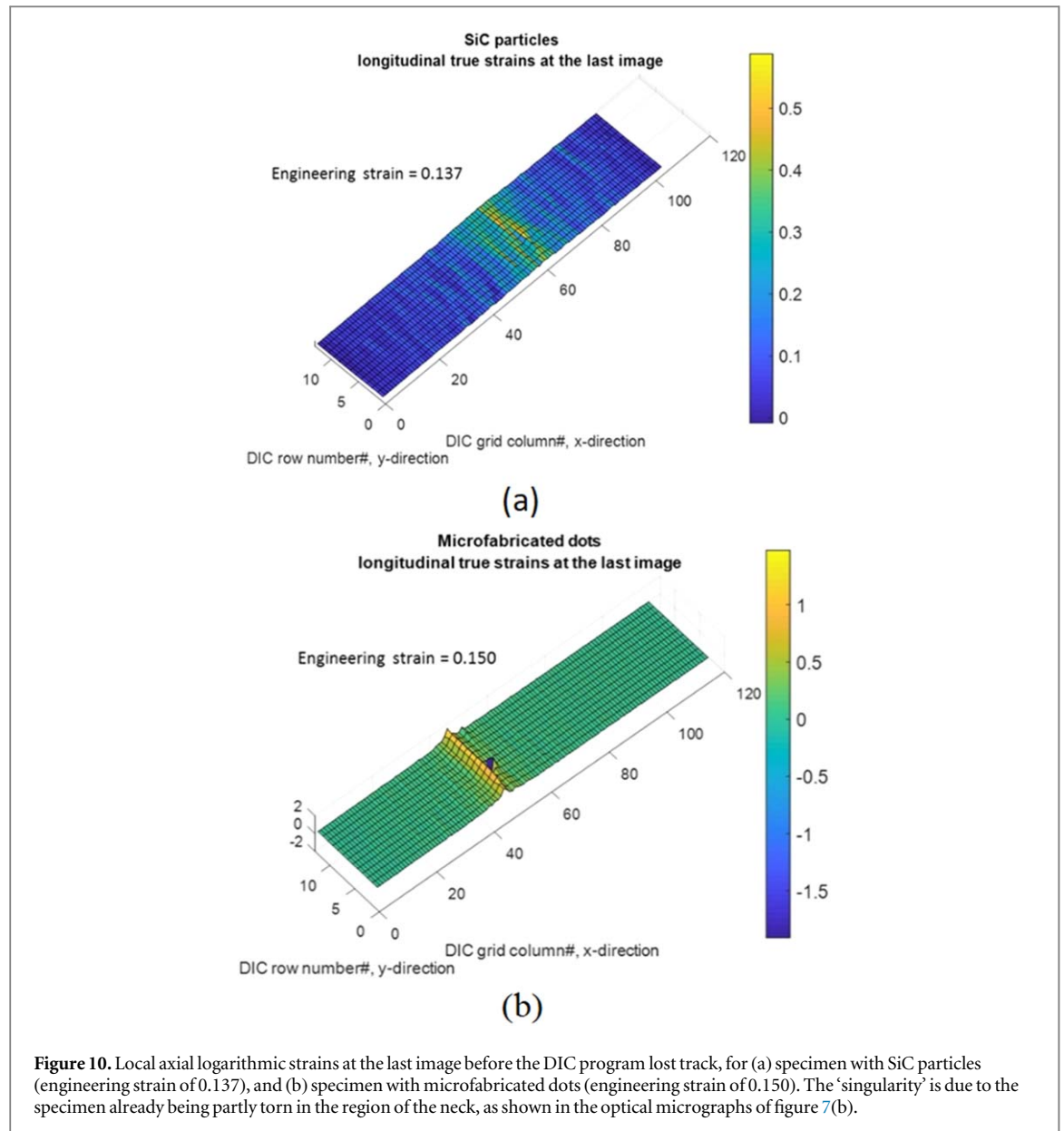
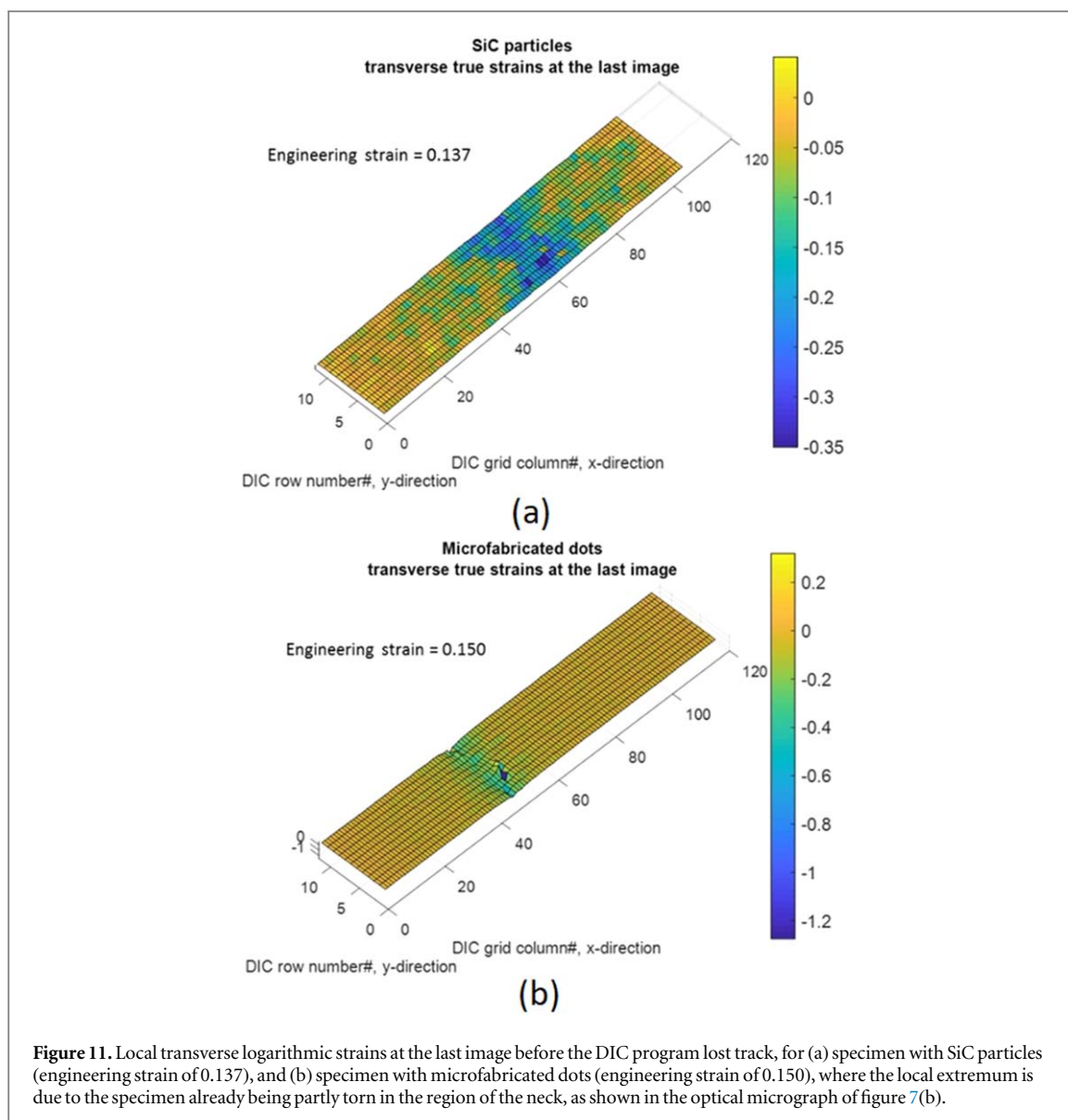


Figure 10. Local axial logarithmic strains at the last image before the DIC program lost track, for (a) specimen with SiC particles (engineering strain of 0.137), and (b) specimen with microfabricated dots (engineering strain of 0.150). The 'singularity' is due to the specimen already being partly torn in the region of the neck, as shown in the optical micrographs of figure 7(b).

Note that most of the recent papers in the literature that used DIC for strain measurement of various MEMS materials including LIGA alloys (mentioned in the introduction) did not map the whole gauge sections as we have done here, but only a portion of their gauge sections, due in part to the difficulty in producing speckle patterns suitable for DIC over the whole specimen. The present technique of using microfabricated thin film fiducial markers potentially provides a reliable way to obtain full-field strains across the whole specimen, regardless of geometry and with a high degree of pattern control and reproducibility over many specimens. A clear advantage would be that this technique can be easily adapted to the needs of specific experiments, such as by adjusting the speckle pattern to improve DIC resolution through the use of smaller, more closely spaced spots, or by having a simple rough pattern that is sufficient just to measure global strain.

However, one disadvantage of this technique is the need for microfabrication facilities. This is generally not a drawback for materials that are already made via wafer-level microfabrication, such as typical MEMS films including LIGA alloys. For specimens that are not made by wafer-level microfabrication, such as those cut from bulk materials, the Au pattern could in principle be deposited through a microfabricated shadow mask. Such a shadow mask could be fabricated, for example, by etching a pattern of through-holes in a thick film on a silicon wafer, and then etching away the silicon in the center of the wafer leaving behind the freestanding patterned shadow mask that is supported by a silicon frame.



4. Conclusion

Thin film Au dots were deposited and photolithographically patterned on freestanding 200 μm -thick LIGA Ni-10%Co tensile specimens with highly polished surfaces, to create fiducial markers for full-field strain measurement via DIC. The dots, drawn in the photolithographical mask, were designed with random orientation and spacing, and their fabrication was the last step in the commercial LIGA process before releasing the specimens from the wafer. The microengineered fiducial markers outperformed several other surface preparation approaches we explored for two-dimensional strain mapping: Applying paint to the grip sections was suitable for measuring engineering strain only. Airbrushing the specimens enabled DIC on the gauge sections, but reproducibility between specimens and control of the thickness of the paint layer to prevent influence on mechanical behavior was an issue. Applying SiC micro particles resulted in higher contrast than the paint and airbrushing approach and less potential for influencing the specimen's mechanical response but achieving a uniform density of the pattern was challenging, as was reproducing the quality of the pattern from one specimen to another. These challenges were resolved by use of the microengineered fiducial markers. A custom DIC program was used and compared to a commercial software, as well as to a known simulated strain created by numerical image stretch and was found to produce very similar results to both. The microfabricated dots enabled two-dimensional surface strain mapping of the entire gauge length of the LIGA tensile specimens. The strain maps showed expected tensile behavior. Compared to the particles approach, the microfabricated dots produced more uniform strain fields and enabled the DIC program to track the full-field displacements to larger deformations. The fiducial marker pattern is replicated exactly for all specimens as it is drawn directly into the photolithographical mask, thus leading to greater reproducibility in the strain measurements, and the

technique is tailorable to specimens of different sizes and desired spatial resolutions. This approach also eliminates the need for post-processing (such as painting) of the fragile as-fabricated specimens, thus reducing potential for specimen damage that could affect the measured properties. (Photolithographically defined micro fiducial markers could in principle also be used as a post-processing surface preparation method by deposition through a shadow mask.) We have thus found thin film microfabricated fiducial markers to be useful for creating suitable and reproducible speckle patterns for DIC, to enable more detailed studies of the mechanical behavior of LIGA Ni alloys.

Acknowledgments

The authors thank Frank DelRio and Nick Barbosa for valuable discussions and support. This work was partially supported by the U.S. Army Combat Capabilities Development Command Armaments Center (CCDC AC) and the Joint Fuze Technology Program (JFTP) under project number 14-G-006, Micro Scale Materials and Energetic Effects Characterization. Specific commercial equipment, instruments, and materials that are identified in this report are listed in order to adequately describe the experimental procedure and are not intended to imply endorsement or recommendation by the National Institute of Standards and Technology (NIST).

Data availability statement

The data generated and/or analysed during the current study are not publicly available for legal/ethical reasons but are available from the corresponding author on reasonable request.

ORCID iDs

Li-Anne Liew  <https://orcid.org/0000-0003-0202-026X>

David T. Read  <https://orcid.org/0000-0003-1479-1619>

May L. Martin  <https://orcid.org/0000-0002-5153-9597>

References

- [1] Becker E W, Ehrfeld W, Hagmann P, Maner A and Munchmeyer D 1986 Fabrication of microstructures with high aspect ratios and great structural heights by synchrotron radiation lithography, galvanoformung, and plastic moulding (LIGA Process) *Microelec. Eng.* **4** 35–6
- [2] Ehrfeld W 1990 The LIGA Process for Microsystems *Micro System Technologies 90* ed H Reichl (Berlin, Heidelberg: Springer) (https://doi.org/10.1007/978-3-642-45678-7_73)
- [3] Guckel H, Christenson T R, Skrobis K J, Denton D D, Choi B, Lovell E G, Lee J W, Bajikar S S and Chapman T W 1990 Deep X-ray and UV lithographies for micromechanics *IEEE 4th Technical Digest on Solid-State Sensor and Actuator Workshop (Hilton Head Island, SC)* 118–22
- [4] Christenson T R and Guckel H 1995 Deep x-ray lithography for micromechanics *Proc. SPIE* **2639** (Micromachining and Microfabrication Process Technology) 134–45
- [5] Haque M A and Saif M T A 2003 A review of MEMS-based microscale and nanoscale tensile and bending testing *Exp. Mech.* **43** 248–55
- [6] Hemker K J and Sharpe W N Jr 2007 Microscale characterization of mechanical properties *Annual Review of Materials Research* 37 (PALO ALTO, CA 94303-0139 USA: Annual Reviews) 93–126
- [7] Gianloa D S and Eberl C 2009 Micro- and nanoscale tensile testing of materials *JOM* **61** 24–35
- [8] Sharpe W N Jr 1982 Applications of the interferometric strain/displacement gage *Opt. Eng.* **21** 483–8
- [9] Sharpe W.N. and McAleavey A 1998 Tensile properties of LIGA nickel *Proc. SPIE* 3512 (Materials and Device Characterization in Micromachining) (SANTA CLARA, CA, SEP 21-22, 1998) 130–1370-8194-2971-6
- [10] Christenson T R, Buchheit T E, Schmale D T and Bourcier R J 1998 Mechanical and metallographic characterization of LIGA fabricated nickel and 80%Ni-20%Fe permalloy *Proc. MRS Symp.* **518** 185–90
- [11] Schwaiger R, Reszat J-T, Bade K, Aktaa J and Kraft O 2009 A combined microtensile testing and nanoindentation study of the mechanical behavior of nanocrystalline LIGA Ni-Fe *Int. J. Mater. Res (formerly Z. Metallkd.)* **100** 68–75
- [12] Liu Y, Ballarini R and Eppell S J 2016 Tension tests on mammalian collagen fibrils *Interface Focus* **6** 20150080
- [13] Buchheit T E, LaVan D A, Michael J R, Christenson T R and Leith S D 2002 Microstructural and mechanical properties investigation of electrodeposited and annealed LIGA nickel structures *Metall. Mater. Trans. A* **33** 539–54
- [14] Sutton M A, Orteu J J and Schreier H 2009 *Image Correlation for Shape, Motion and Deformation Measurements: Basic Concepts, Theory and Applications* (U.S: Springer) (<https://doi.org/10.1007/978-0-387-78747-3>)
- [15] Pan B, Qian K, Xie H and Asundi A 2009 Two-dimensional digital image correlation for in plane displacement and strain measurement: a review *Meas. Sci. Tech.* **20** art no062001
- [16] Kammers A D and Daly S 2011 Small-scale patterning methods for digital image correlation under scanning electron microscopy *Meas. Sci. Technol.* **22** art. no.125501
- [17] Chasiotis I and Knauss W G 2002 A new microtensile tester for the study of MEMS materials with the aid of atomic force microscope *Exp. Mech.* **42** 51–7

- [18] Roland T, Arscott S, Sabatier L, Buchaillot L and Charkaluk E 2011 Digital image correlation of metal nanofilms on SU-8 for flexible electronics and MEMS *J. Micromech. Microeng.* **21** 125005
- [19] Robin C J, Vishnoi A and Jonnalagadda K N 2014 Mechanical behavior and anisotropy of spin-coated SU-8 thin films for MEMS *J MEMS* **23** 168–80
- [20] Naraghi M, Ozkan T, Chasiotis I, Hazra S S and de Boer M P 2010 MEMS platform for on-chip nanomechanical experiments with strong and highly ductile nanofibers *J. Micromech. Microeng.* **20** 125022
- [21] Jonnalagadda K N, Chasiotis I, Yagnamurthy S, Lambros J, Pulskamp J, Polcawich R and Dubey M 2010 Experimental investigation of strain rate dependence of nanocrystalline Pt films *Exp. Mech.* **50** 25–35
- [22] Banks-Sills L, Shklovsky J, Krylov S, Bruck H A, Fourman V, Eliasi R and Ashkenazi D 2011 A methodology for accurately measuring mechanical properties on the micro-scale *Strain* **47** 288–300
- [23] Scrivens W A, Luo Y, Sutton M A, Collette S A, Myrick M L, Miney P, Colavita P E, Reynolds A P and Li X 2007 Development of patterns for digital image correlation measurements at reduced length scales *Exp. Mech.* **47** 63–77
- [24] Li N, Guo S and Sutton M A 2011 Recent progress in e-beam lithography for SEM patterning *MEMS and Nanotechnology, Vol. 2, Conf. Proc. Soc. Exp. Mech., Series ed T Proulx 2* (New York: Springer) 163–166
- [25] Berfield T A, Patel J K, Shimmin R G, Braun P V, Lambros J and Sottos N R 2007 Micro- and nanoscale deformation measurement of surface and internal planes via digital image correlation *Exp. Mech.* **27** 51–62
- [26] Ruggles T.J., Bomarito G.F., Cannon A.H. and Hochhalter J.D. 2017 Selectively Electron-Transparent Microstamping Toward Concurrent Digital Image Correlation and High-Angular Resolution Electron Backscatter Diffraction (EBSD) Analysis *Microscopy and Microanalysis* **23** 1091-1095
- [27] Collins J G, Wright M C and Muhlstein C L 2011 Cyclic stabilization of electrodeposited nickel structural films *J. Microelectromech. Syst.* **20** 753–63
- [28] Sharon J A, Padilla H A II and Boyce B L 2013 Interpreting the ductility of nanocrystalline metals *J Mat Res* **28** 1539–52
- [29] Suresha S J, Haj-Taieb M, Bade K, Aktaa J and Hemker K J 2010 The influence of tungsten on the thermal stability and mechanical behavior of electrodeposited nickel MEMS structures *Scripta Mat* **63** 1141–4
- [30] Liew L A, Read D T, White R M and Barbosa N 2018 U.S. Army ARDEC Joint Fuze Technology Program (JFTP) Task 2 report: quasi-static tensile tests of microfabricated electrodeposited (LIGA) Ni alloys *NIST Interagency/Internal Report (NISTIR), National Institute of Standards and Technology, Gaithersburg, MD, [online]* **8182** 1-108 www.nist.gov
- [31] Liew L A, Read D T, Martin M L, DelRio F W, Bradley P E, Barbosa N, Christenson T and Geaney J 2020 Elastic-plastic properties of mesoscale electrodeposited LIGA nickel alloys films: microscopy and mechanics (2020) *J. Micromech. Microeng.* **31** 015002
- [32] Martin M L, Liew L A, Read D T, Christenson T, DelRio F and Geaney J 2020 Dominant factors for fracture at the microscale in electrodeposited nickel alloys *Sens. Actuators A* **314** 112239
- [33] Abramoff M D, Magalhaes P J and Ram S J 2004 Image Processing with ImageJ *Biophotonics International* **11** 36–42
- [34] VIC-2D, Correlated Solutions, Inc.: (<https://correlatedsolutions.com/vic-2d/>)
- [35] Hencky H 1928 Über die form des Elastizitätsgesetzes bei ideal elastischen Stoffen *Zeitschrift für technische Physik.* **9** 215–20